Appl. Phys. A 66, 487–491 (1998)

Applied Physics A
Materials
Science & Processing

Pressure effects during pulsed-laser deposition of barium titanate thin films

J. Gonzalo[1], R. Gómez San Román[2], J. Perrière[3], C.N. Afonso[1], R. Pérez Casero[2]

[1] Instituto de Optica, CSIC, Serrano 121, 28006 Madrid, Spain
(Fax: +34-1/5645-557, E-mail: iodfv30@pinar1.csic.es)
[2] Departamento de Física Aplicada C-XII, Universidad Autónoma de Madrid, 28049 Cantoblanco, Madrid, Spain
[3] Groupe de Physique des Solides, Universités Paris VII et VI, URA 17 du CNRS, Tour 23, 2 Place Jussieu, 75251 Paris Cedex 05, France

Received: 7 November 1997/Accepted: 8 November 1997

Abstract. The composition and homogeneity of barium titanate films grown by pulsed-laser deposition at different substrate temperatures (room temperature, 700 °C) and gas environments (O_2, Ar) in a broad pressure range (10^{-7}–1 mbar) are correlated to the plasma expansion dynamics. It is found that the deposited films present an excess of Ba in the intermediate pressure range ($10^{-2} < P < 10^{-1}$ mbar) and a peaked distribution of Ba to Ti atoms ratio, that is not related to either the substrate temperature or the nature of the gas environment. The results are discussed in terms of the dependence of the plume length (L_P) on the gas pressure and the existence of scattering processes for distances (d) from the target lower than L_P and the diffusion of the ejected species for $L_P < d$.

PACS: 81.15 Fg; 77.84 Dy; 78.47 +p

Barium titanate ($BaTiO_3$) is a promising material for the fabrication of opto-electronic integrated devices such as non-volatile random-access memories, thin film capacitors, or infrared sensors [1], that require high-quality crystalline and oriented films with smooth surfaces. Nevertheless, although different techniques have been used to date to grow $BaTiO_3$ thin films, for example molecular beam epitaxy [2], rf sputtering [3], plasma-enhanced MOCVD [4], sol–gel [5], and pulsed laser deposition (PLD) [1, 6–10], the deposited $BaTiO_3$ films are in some cases amorphous or polycrystalline and may even present a non-ferroelectric cubic phase.

Among all the deposition methods PLD is a very promising technique because of its ability to grow stoichiometric films of complex oxides in reactive environments, provided suitable experimental conditions are used. In fact, it has been reported that it is possible to grow highly oriented $BaTiO_3$ films, although the substrate temperature (T_S) and the oxygen background pressure appear as critical parameters that determine the final step of the film formation [1, 6–8, 10]. T_S determines the amorphous or crystalline character of the deposited films, whereas the presence of an O_2 environment not only has an influence on the crystalline structure when growing films at high T_S, but it may also ease the formation of volatile oxides during the film deposition. These volatile oxides may be re-evaporated from the growing film and therefore modify the film composition [1, 11]. In addition, prior to the arrival of the ejected species at the substrate, the presence of a gas environment has a strong influence on the expansion of the laser-produced plasma. It modifies the kinetic energy [12–15] and the spatial distribution of the ejected species present in the plasma [12, 16–18], and it may also induce compositional changes in the deposited films [1, 12, 17]. Therefore, a more complete understanding of the influence of the different deposition parameters on the structural and physical properties of the films is required.

The aim of this work is then to correlate the stoichiometry and material distribution of the deposited films with the plasma expansion dynamics in a broad pressure range. The composition, homogeneity and crystalline structure of the films were analysed by Rutherford backscattering spectrometry (RBS) and X-ray diffraction (XRD), and spatially resolved real-time optical emission spectroscopy was used to study the nature and dynamics of the species present in the plasma. The results are analysed in terms of the expansion dynamics of the plasma and the interaction processes between the ejected species and the gas atoms or molecules.

1 Experimental

Laser ablation of a rotating $BaTiO_3$ ceramic target was performed by using either a frequency-quadrupled Nd:YAG laser ($\lambda = 266$ nm, $\tau = 7$ ns FWHM) or an ArF excimer laser ($\lambda = 193$ nm, $\tau = 12$ ns FWHM). The target was placed in a vacuum chamber evacuated to a residual pressure of 10^{-7} mbar and the selected laser beam was focused onto the target surface at an incident angle of 45°. Films were grown in a broad pressure range (10^{-7} to 1 mbar) either in O_2 or Ar environments. In the case of the Nd:YAG ablation, the films were grown on MgO substrates held at 700 °C and placed 3.5 cm from the target surface. In the case of the ArF ablation, films were grown on Si(100) substrates held at room temperature (RT) and placed at 3.1 cm from the target surface. In both cases, the laser energy density was 2 J/cm^2 and the repetition rate 5 Hz.

The plasma formed during the ArF laser ablation of the $BaTiO_3$ target was imaged with $\times 2$ magnification onto the entrance slit of a spectrometer (SPEX, 0.05-nm resolution). The plasma emission was analysed at different distances from the target (0.4, 1.3, 1.5, and 2.0 cm) as a function of the gas pressure, the spatial resolution being 130 μm. The emitted light was collected by a photomultiplier (15-ns rise time), connected to a 500 MHz digitizer for transient emission measurements. Further details of the experimental setup can be found elsewhere [12, 13, 18].

Nuclear microanalysis was used to study the elemental composition of the deposited films. The depth distribution of Ba and Ti cations and the film thickness were determined by Rutherford backscattering spectrometry (RBS) using a $^4He^+$ beam and by simulating the results with the RUMP program [19]. X-ray diffraction with a Cu K_α radiation was used in the $\theta - 2\theta$ Bragg–Brentano geometry to determine the crystallographic structure of the films deposited on MgO at $T_S = 700\,^\circ C$ and the nature of the phases formed.

2 Results

Figure 1a shows the dependence of the relative content of Ba ($C_{Ba} = N_{Ba}/(N_{Ba} + N_{Ti})$) on the oxygen pressure of films grown on heated (700 °C) MgO substrates. The plotted values correspond to the thicker region of the films. The relative content of Ba is close to that of the ideal composition of $BaTiO_3$ ($C_{Ba} = C_{Ti} = 0.5$) for films grown either at low ($P \leq 10^{-2}$ mbar) or high ($P \geq 2 \times 10^{-1}$ mbar) oxygen pressures, whereas the films show a large Ba excess in the intermediate pressure range, C_{Ba} being a maximum ($C_{Ba} = 0.58$) for films grown at $\approx 10^{-1}$ mbar.

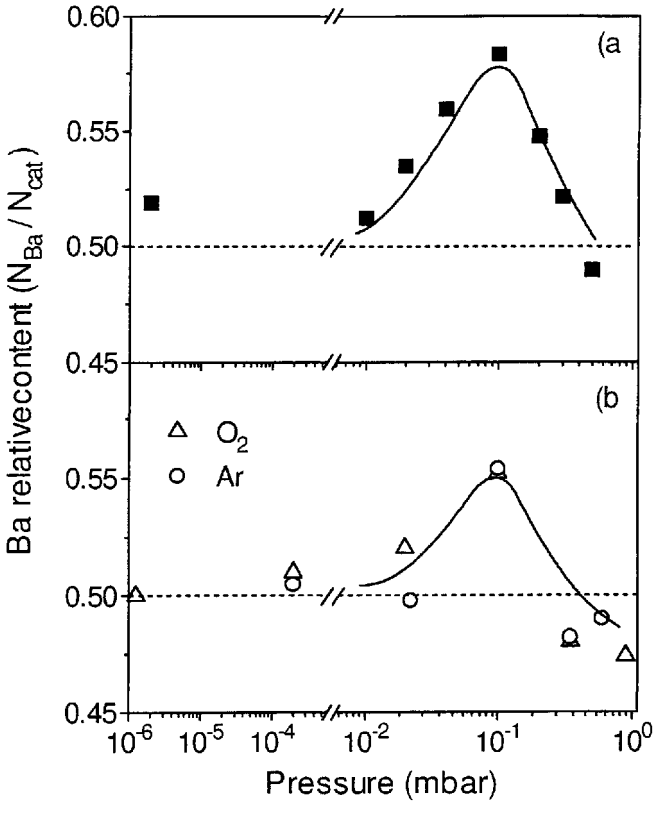

Fig. 1a,b. Barium relative content ($N_{Ba}/N_{Ba} + N_{Ti}$) as a function of the gas pressure of films deposited **a** in O_2 on heated (700 °C) MgO substrates and **b** in O_2 (△) or argon (○) on Si substrates at room temperature. The Ba relative content is measured at the thicker region of the films and the *lines* are only a guide

The composition and structural characteristics of laser-deposited barium titanate films might depend on the combined effect of the substrate temperature (T_S) and the gas pressure. Therefore, in order to study the process responsible for the Ba excess observed in the intermediate pressure range, films were grown on Si substrates held at RT either in O_2 or in an inert (Ar) environment. Figure 1b shows the dependence of the Ba relative content (C_{Ba}) on the gas pressure. No significant differences are observed in the results obtained either in O_2 or Ar. Furthermore, comparison of Fig. 1a and Fig. 1b shows that the Ba relative content follows a similar pattern of behaviour to that observed for the in situ high-temperature grown films: the composition differs from the stoichiometric one only for films grown in the intermediate pressure range.

The presence of a gas environment during the film deposition also induces a change in the angular dependence of the film composition, as it can be seen in Fig. 2 for the C_{Ba}/C_{Ti} ratio for films deposited on Si substrates held at room temperature. Similar qualitative results are obtained in O_2 (Fig. 2a) and Ar (Fig. 2b) environments. Films deposited at low pressures ($\approx 10^{-4}$ mbar) show an almost constant C_{Ba}/C_{Ti} ratio at all measured angles. When the gas pressure is increased to the critical value of $\approx 10^{-1}$ mbar, the C_{Ba}/C_{Ti} ratio of the deposited films is no longer uniform and shows a maximum at the centre of the distribution. Finally, films grown at higher gas pressures (≈ 6–9×10^{-1} mbar) show an angular dependence on the C_{Ba}/C_{Ti} ratio similar to that obtained in vacuum, but with a slightly lower Ba relative content.

The absence of any significant effects related to the nature of the gas was checked further by growing films at an elevated substrate temperature (700 °C) either in O_2 or Ar environments. The crystalline structure of the films was studied by X-ray diffraction and Fig. 3 shows two typical X-ray spectra obtained for films deposited in O_2 and Ar at 0.5 mbar. In

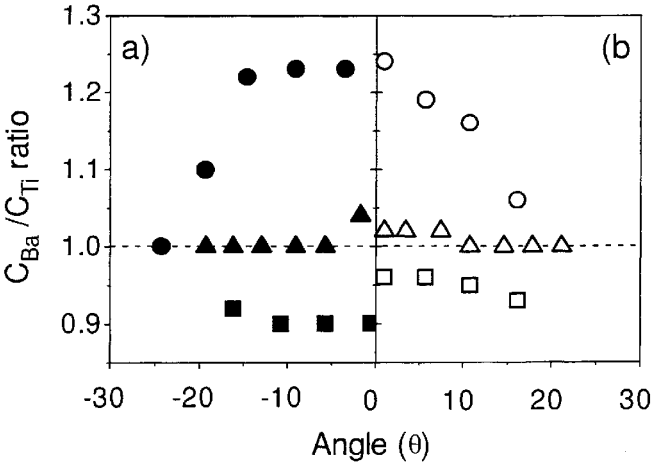

Fig. 2a,b. Angular distribution of the barium to titanium ratio (C_{Ba}/C_{Ti}) of films deposited on Si substrates at room temperature **a** in O_2 (▲, ●, ■) and **b** in argon (△, ○, □) environments at (▲, △) 2.4×10^{-4} mbar, (●, ○) 1.0×10^{-1} mbar, (■) 9.0×10^{-1} mbar, and (□) 6.0×10^{-1} mbar

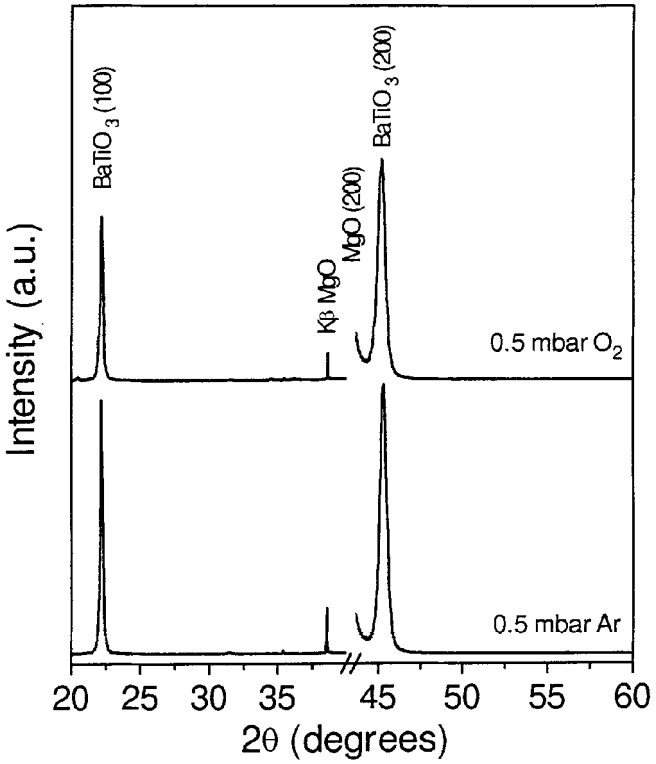

Fig. 3. XRD diffraction spectra for films deposited on heated (700 °C) MgO substrates in 5.0×10^{-1} mbar of O_2 and argon

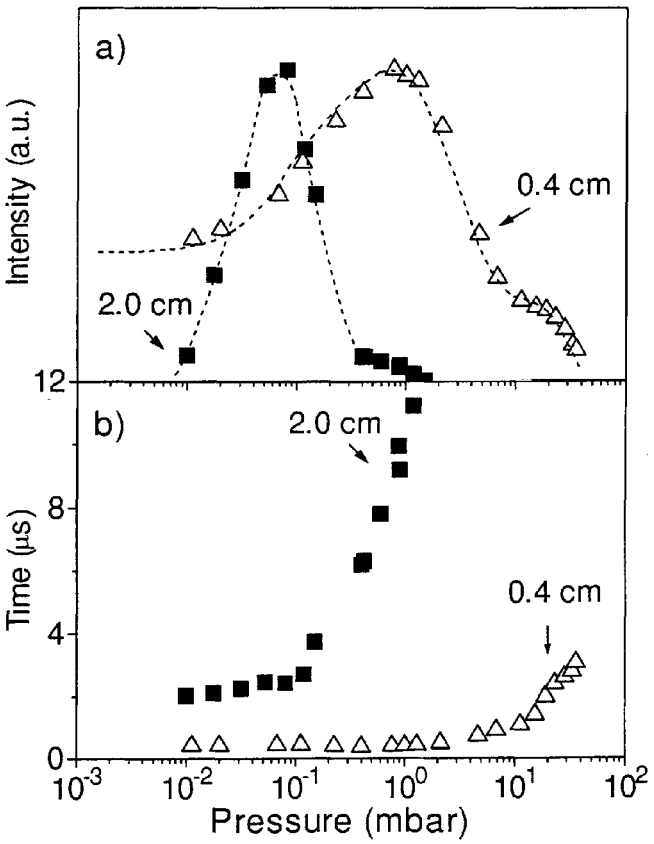

Fig. 4. a Maximum emission intensity (I_M) and **b** its delay with respect to the laser pulse (t_M) as a function of the O_2 pressure applied. The results are recorded at (△) 0.4 cm and (■) 2.0 cm from the target surface and correspond to the Ba* emission at 553.6 nm. For ease of comparison, the data plotted in **a** have been normalized to the maximum intensity measured at each distance. The *dashed lines* in **a** are only a guide

both cases, the two main peaks detected were identified as the (100) and (200) diffraction lines characteristic of the $BaTiO_3$ phase, thus indicating that the deposited films are strongly textured, with their *c* axis oriented along the direction perpendicular to the substrate surface.

Finally, in order to analyse the influence that the presence of a gas environment has on the plasma expansion dynamics, we have studied the plasma emission by using optical emission spectroscopy. The emission spectra from the $BaTiO_3$ laser-produced plasma was studied in the wavelength range 390–600 nm and in different environments: vacuum, O_2, and Ar. No emission from excited oxidised species (BaO* or TiO*) could be detected. The observed emission lines correspond to neutrals (Ba*, Ti*) or ions (Ba^{+*}, Ti^{+*}) and were identified according to standard tabulations [20]. In this study the Ba^{+*} (493.4 nm), Ti^{+*} (439.5 nm), Ba* (553.6 nm), and Ti* (394.9 nm) emission lines were considered. However, since the gas pressure has a similar effect on the emission characteristics of the different lines, only results related to the Ba* emission line are presented. Further details of the plasma expansion kinetics can be found elsewhere [13].

Figure 4 shows the dependence of the maximum transient emission intensity (I_M) (Fig. 4a) and its delay with respect to the laser pulse (t_M) (Fig. 4b) on the O_2 pressure for the Ba* emission line at two distances from the target surface (0.4 and 2.0 cm). For ease of comparison, the values of I_M presented in Fig. 4a have been normalised to the maximum intensity recorded for the emission at each distance. It is observed how I_M increases with the oxygen pressure up to a maximum value that depends on the distance to the target, and then decreases sharply to zero for higher pressures. The pressures at which the maximum I_M is observed and at which I_M becomes zero also depend on the distance to the target; the higher the distance, the lower the pressure. At 0.4 cm the emission is detected in the whole range (10^{-7} to 20 mbar), but at 2.0 cm the range is much narrower (10^{-3} to 1 mbar). Figure 4b shows that t_M remains constant and similar to the value measured in vacuum up to a pressure threshold that again depends on the distance to the target, whereas at higher pressures t_M increases sharply. Similar features were observed for the different emission lines considered in either O_2 or Ar environments.

3 Discussion

The high-temperature in situ growth of oxide films by PLD depends not only on the incident flux of the various species reaching the substrate, but also on the atomic phenomena taking place at the surface of the growing films. In general, the flux of the species arriving at the substrate depends either on the laser–target interaction, which may determine the nature of the ejected species [18, 21], or on the plasma expansion dynamics, mainly determined by the gas pressure [9, 12–15]. On the other hand the processes taking place at the surface of the growing film, which determine the nature and stability domain of the crystalline phases formed in the deposited ma-

terial, are related to the substrate temperature (T_S) and the gas pressure (generally O_2) [1, 10, 11].

The results presented in Figs. 1a and 1b show that films with similar composition are obtained when growing films either at 700 °C or RT, the film composition being dependent only on the gas pressure. Moreover, the reactive character of the O_2 environment does not play an essential role, since amorphous films with similar composition (Fig. 1b) and angular distribution (Fig. 2) are obtained at RT, and textured crystalline films (Fig. 3) are obtained at 700 °C, in either O_2 or Ar environments. Therefore, the results above presented suggest that the changes observed in the film composition should not be related to either the substrate temperature or to the gas nature. They are related instead to the changes observed in the plasma expansion process that takes place when the pressure of the gas environment is increased. The increase in t_M observed when the gas pressure is increased (Fig. 4b) evidences that the presence of a gas environment produces the deceleration of the species present in the plasma, because of the interaction of the ejected species with the atoms or molecules of the gas environment. If the pressure is high enough, the gas environment may confine the plasma to a finite region [13, 14, 21], as is suggested in our experiments by the high value of t_M at $d = 2.0$ cm when the gas pressure is increased ($t_M \approx 12\,000$ ns at 1 mbar) (Fig. 4b) and by the fact that the range of distances from the target surface at which the emission is observed decreases when the gas pressure is increased (Fig. 4a). If we consider that the plasma expands adiabatically once the laser pulse has ended, it is possible to estimate the plume length according to the expression [22]:

$$L_p = A\,[(\gamma-1)E]^{1/(3\gamma)}\,P^{-1/(3\gamma)}V^{(\gamma-1)/(\gamma-3)}\,, \qquad (1)$$

where A is a geometrical factor related to the shape of the laser spot at the target surface, γ is the ratio of specific heats (C_p/C_v), E is the laser energy per pulse, P is the gas pressure, and V is the initial volume of the plasma ($V \approx v_0\tau \times$ spot size, v_0 being the initial species velocity and τ the laser pulse duration). For a given set of experimental conditions A, E, and V are fixed and γ can be estimated to be in the range 1.3–1.4 [22]. Therefore it is possible to rewrite (1) in the form:

$$L_p = CP^{-1/(3\gamma)}\,, \qquad (2)$$

where C is a parameter that only depends on the experimental conditions. In a previous work [9] we showed that for a given distance to the target (d), it is possible to estimate L_P experimentally from Fig. 4 by assuming that $L_P \approx d$ for the pressure at which $I_M(d)$ becomes zero. The experimental and the calculated values obtained from (1) are plotted in Fig. 5 as a function of the O_2 pressure and the agreement is very good. The extrapolation of the calculated curve shows clearly that for our target–substrate distance (d_{TS}) and gas pressures below 10^{-1} mbar, the plume length is longer than the target–substrate distance ($L_P > d_{TS}$), whereas the opposite ($L_P < d_{TS}$) is true for higher pressures. Therefore, the film growth regime will be different for films grown at pressures below and above $\approx 10^{-1}$ mbar. This value is in excellent agreement with the pressure at which the Ba relative content has a maximum value as was shown in Fig. 1.

In the pressure range in which the films were grown ($P \leq 1$ mbar) the interactions between the ejected species and

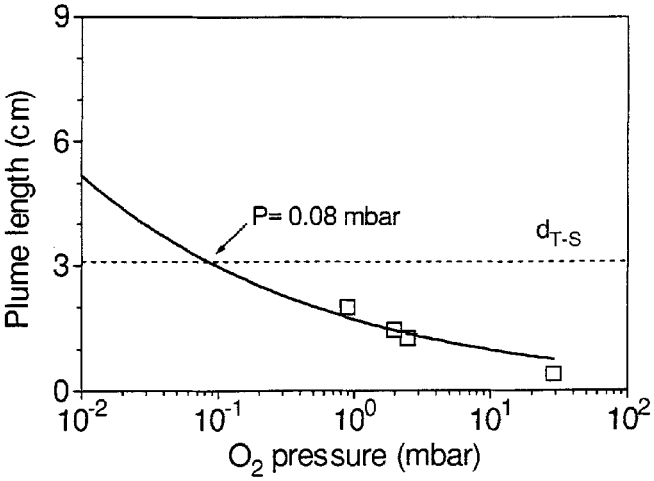

Fig. 5. Plume length (L_P) determined experimentally from the (□) Ba* emission at 553.6 nm as a function of the O_2 pressure. The *full line* corresponds to the best fit obtained using the adiabatic expansion model ($L_P = CP^{-1/3\gamma}$, where $\gamma = 1.4$ and $C = 1.7$). The target–substrate distance (d_{TS}) used in the experiment (3.1 cm) is marked as a *dashed line*

the gas atoms or molecules have been understood in terms of the scattering of the ejected species by the gas atoms or molecules [12, 14, 16–18]. In this case, the effect of the gas environment on the angular distribution of the deposited material film composition should be related to the mass and size of the species present in the plasma. Assuming that the plasma is mainly formed by atomic species (Ba and Ti) and considering a simple scattering model based on hard spheres [16], it is possible to estimate the mean free path of Ba or Ti atoms in O_2 according to the expression [23]:

$$\lambda_1 = k_B T/\pi P d_{12}^2\,, \qquad (3)$$

where k_B is the Boltzmann constant, T is the temperature of the gas, P is the gas pressure, and $d_{12} = (r_1 + r_2)$ is the impact parameter (r_1 and r_2 being the radii of the species 1 and 2). Taking into account the masses and atomic radii of Ba, Ti, and O_2 [24] ($m_{Ti} = 48$, $m_{Ba} = 134$, $r_{O_2} = 1.8$ Å, $r_{Ti} = 2.0$ Å, and $r_{Ba} = 2.8$ Å) it is possible to estimate the mean free path of Ba (λ_{Ba}) and Ti (λ_{Ti}) species in an O_2 pressure. At low pressures ($P < 10^{-2}$ mbar) the values of λ_{Ba} and λ_{Ti} are of the same order or even larger than the target–substrate distance ($d_{TS} = 3.1$ cm). Therefore, the scattering probability is very low and the expansion velocity of the ejected species will be similar to the observed in vacuum. This means that the value of t_M should remain very close to that measured in vacuum in agreement with the experimental results plotted in Fig. 4b. Furthermore, assuming that the sticking coefficient of each element is equal to unity, the atomic composition measured in the deposited films can be reasonably considered as a measurement of the flux of the incident species, and therefore the angular distribution and composition of the deposited material should be similar to those of films grown in vacuum (Figs. 1 and 2). When the gas pressure is increased λ_{Ba} and λ_{Ti} decrease and the effect of the gas environment becomes significant. At the pressure of 10^{-1} mbar, when $L_P \approx d_{TS}$, the calculated mean free paths are $\lambda_{Ba} \approx 0.08$ cm and $\lambda_{Ti} \approx 0.13$ cm. In this case $\lambda_{Ba} \sim \lambda_{Ti} \ll d_{TS}$ and thus the expected number of collisions that the Ba and Ti atoms would

experience is high enough to consider that the dominant effect is that of the masses. Therefore, since $m_{Ba} > m_{Ti}$, a lower broadening of the Ba angular distribution can be expected on the deposited films. In such conditions the relative amount of Ba species that travel along the normal to the target will be higher than that of Ti, thus leading to a maximum in the C_{Ba}/C_{Ti} ratio at the centre of the distribution. This reasoning is in very good agreement with the results shown in Fig. 2. Furthermore, this process depends only on the mass and size of the ejected species and gas atoms or molecules. Thus, since $r_{O_2} \approx r_{Ar}$ and $m_{O_2} = 0.8 m_{Ar}$, the effect should be qualitatively similar in Ar and O_2 environments as is experimentally observed (Figs. 1 and 2).

At higher pressures ($P > 10^{-1}$ mbar) the plume length is smaller than the target–substrate distance ($L_p < d_{TS}$). Therefore, once the ejected species have reached L_p and lost their kinetic energy, they should be transported by diffusion from L_P to the substrate [15, 22]. As a consequence of the scattering suffered by these species at distances shorter than the plume length, their angular distribution at the plume boundary (L_P) is not the same for Ba and Ti as discussed above. Beyond L_p, and since the ejected species have been thermalized [14, 16], their movement between L_p and the substrate is random. Therefore, the species initially having the broader angular distribution (Ti) will provide a higher relative amount of species in the forward direction (i.e. the center of the deposit) as they simulate a planar diffusion slightly better. As a consequence, films grown at pressures above 10^{-1} mbar should exhibit not only a decrease in the thickness, as experimentally observed, but also a decrease of the C_{Ba} at the center of the distribution when compared to the films grown at 10^{-1} mbar, (i.e. when $L_P \approx d_{TS}$). Furthermore, this decrease should be higher for higher pressures as experimentally observed in Fig. 1.

4 Conclusions

The composition and the angular dependence of the Ba/Ti relative content of barium titanate films grown by PLD depend only on the pressure and not on the nature (reactive or inert) of the gas environment. At low gas pressures, the scattering of the ejected species by the gas atoms or molecules is the dominant process that determines the relative Ba/Ti content of the deposited films. At high oxygen pressures, the combination of the initial scattering and the further diffusion that takes place once the ejected species have been thermalized is the process that determines the film composition. The combination of these effects leads to films enriched in Ba and with a peaked angular distribution of Ba to Ti ratio for those pressures for which the plume length is close to the target-substrate distance.

Acknowledgements. J.M. Ballesteros (I. de Optica, Madrid, Spain) is thanked for experimental assistance. This work was partially supported by CICYT (Spain) under TIC 96-0467 and the CNRS (France) GDR No 86.

References

1. R.E. Leuchtner, K.S. Grabowski: In *Pulsed Laser Deposition of Thin Films*, ed. by D.B. Chrisey, G.K. Hubler (Wiley, New York 1994) p. 473
2. R.A. McKee, F.J. Walker, J.R. Conner, E.D. Specht, D.E. Zelmon: Appl. Phys. Lett. **59**, 782 (1991)
3. K. Fujimoto, Y. Kobayashi, K. Kubota: Thin Solid Films **169**, 249 (1989)
4. C.S. Chern, J. Zhao, L. Luo, P. Lu, Y.Q. Li, P. Norris, B. Kear, F. Cosandey, C.J. Maggiore, B. Gallois, B.J. Wilkens: Appl. Phys. Lett. **60**, 1144 (1992)
5. M.N. Kamalasaman, S. Chandra, P.C. Joshi, A. Masingh: Appl. Phys. Lett. **59**, 3547 (1991)
6. D-Y. Kim, S-G. Lee, Y-K. Park, S-J. Park: Jpn. J. Appl. Phys. **34**, L1564 (1995)
7. D.H. Kim, H.S. Kwok: Appl. Phys. Lett. **65**, 3188 (1995)
8. W.J. Lin, T.Y. Tseng, H.B. Lu, S.L. Tu, S.J. Yang, I.N. Lin: J. Appl. Phys. **77**, 6466 (1995)
9. J. Gonzalo, C.N. Afonso, J.M. Ballesteros: Appl. Surf. Sci. **109/110**, 606 (1997)
10. J. Zhang, D. Cui, H. Lu, Z. Chen, Y. Zhou, L. Li, G. Yang, S. Martin, P. Hess: Jpn. J. Appl. Phys. **36**, 276 (1997)
11. D. Roy, S.B. Krupanidhi: J. Mater. Res. **7**, 2521 (1992)
12. J. Gonzalo, C.N. Afonso, F. Vega, D. Martinez García, J. Perrière: Appl. Surf. Sci. **86**, 40 (1995)
13. J. Gonzalo, C.N. Afonso, I. Madariaga: J. Appl. Phys. **81**, 951 (1997)
14. D.B. Geohegan: In *Pulsed Laser Deposition of Thin Films*, ed. by D.B. Chrisey, G.K. Hubler (Wiley, New York 1994) p. 115
15. W.K.A. Kummudumi, Y. Nakayama, Y. Nakata, T. Okada, M. Maeda: J. Appl. Phys. **74**, 7510 (1993)
16. J.C.S. Kools: J. Appl. Phys. **74**, 6401 (1993)
17. K.L. Saenger: In *Pulsed Laser Deposition of Thin Films*, ed. by D.B. Chrisey, G.K. Hubler (Wiley, New York 1994) p. 199
18. J. Gonzalo, C.N. Afonso, J.Perrière: J. Appl. Phys. **79**, 8042 (1996)
19. L.R. Doolittle: Nucl. Instrum. Methods B **9**, 344 (1985)
20. C.E. Moore: NSRDS-NBS Monograph **35** (1975); G.A. Martin, J.R. Fuhr, W.L. Wiese: J. Phys. Chem. Ref. Data **17**, Suppl. 3 (1988)
21. H.F. Sakeek, T. Morrow, W.G. Graham, D.G. Walmsley; J. Appl. Phys. **75**, 1138 (1994)
22. P.E. Dyer, A. Issa, P.H. Key: Appl. Surf. Sci. **46**, 89 (1990)
23. S. Dushman: *Scientific Foundations of Vacuum Technique* (Wiley, New York 1962) chap. 1
24. Periodic Table of Elements (SMI Corp. 1991); R.A. Alberty, R.J. Silbey: *Physical Chemistry* (Wiley, New York 1992) chap. 18